Published in final edited form as:
*Neurorehabil Neural Repair*. 2013 June ; 27(5): 411–420. doi:10.1177/1545968312469835.

# Motor and premotor cortices in subcortical stroke: proton magnetic resonance spectroscopy measures and arm motor impairment

**Sorin C. Craciunas, MD, PhD**[a,1], **William M. Brooks, PhD**[a,c], **Randolph J. Nudo, PhD**[b,d], **Elena A. Popescu, PhD**[a], **In-Young Choi, PhD**[a,c], **Phil Lee, PhD**[a,d], **Hung-Wen Yeh, PhD**[e], **Cary R Savage, PhD**[f], and **Carmen M. Cirstea, MD, PhD**[a,c,g,*]

[a]Hoglund Brain Imaging Center, University of Kansas Medical Center

[b]Landon Center on Aging; Departments of, University of Kansas Medical Center

[c]Neurology, University of Kansas Medical Center

[d]Molecular and Integrative Physiology, University of Kansas Medical Center

[e]Biostatistics, University of Kansas Medical Center

[f]Psychiatry and Behavioral Sciences, University of Kansas Medical Center

[g]Physical Therapy and Rehabilitation Science, University of Kansas Medical Center

## Abstract

**Background—**Although functional imaging and neurophysiological approaches reveal alterations in motor and premotor areas after stroke, insights into neurobiological events underlying these alterations are limited in human studies.

**Objective—**We tested whether cerebral metabolites related to neuronal and glial compartments are altered in the hand representation in bilateral motor and premotor areas and correlated with distal and proximal arm motor impairment in hemiparetic persons.

**Methods—**In twenty participants at >6 months post-onset of a subcortical ischemic stroke and sixteen age and sex-matched healthy controls, the concentrations of N-acetylaspartate and myoinositol were quantified by proton magnetic resonance spectroscopy ($^1$H-MRS). Regions of interest, identified by functional MRI, included primary (M1), dorsal premotor (PMd), and supplementary (SMA) motor areas. Relationships between metabolite concentrations and distal (hand) and proximal (shoulder/elbow) motor impairment using Fugl-Meyer Upper Extremity (FMUE) subscores were explored.

**Results—**N-acetylaspartate was lower in M1 (p=0.04) and SMA (p=0.004) and myo-inositol was higher in M1 (p=0.003) and PMd (p=0.03) in the injured (ipsilesional) hemisphere after stroke compared to the left hemisphere in controls. N-acetylaspartate in ipsilesional M1 was positively correlated with hand FMUE subscores (p=0.04). Significant positive correlations were also found between N-acetylaspartate in ipsilesional M1, PMd, and SMA and in contralesional M1 and shoulder/elbow FMUE subscores (p=0.02, 0.01, 0.02 and 0.02 respectively).

[*]*Corresponding author* Hoglund Brain Imaging Center University of Kansas Medical Center 3901 Rainbow Blvd Mail Stop 1052 Kansas City, Kansas US, 66160 Tel: (913) 588-4373 Fax: (913) 588-9071 .
[1]*Present address*: Neurosurgery Department IV, Bagdasar-Arseni Hospital

**Conclusions—**Our preliminary results demonstrated that $^{1}$H-MRS is a sensitive method to quantify relevant neuronal changes in spared motor cortex after stroke, and consequently increase our knowledge of the factors leading from these changes to arm motor impairment.

### Keywords

subcortical stroke; motor and premotor cortices; proton magnetic resonance spectroscopy; distal and proximal arm motor impairment

## Introduction

Human imaging studies have revealed that early after subcortical stroke, restoration of paretic arm function is associated with a greater involvement of radiologically normal-appearing (or spared) motor (primary motor cortex or M1) and premotor (dorsal premotor cortex or PMd, supplementary motor area or SMA) areas in both injured (ipsilesional) and un-injured (contralesional) hemispheres[1-3]. Later, successful recovery occurs in stroke survivors who exhibit relatively normal patterns of ipsilesional activation and less contralesional motor activation, whereas patients, who often show bilateral cortical activation, typically have less complete recovery[4-6]. These results should be viewed in the context of the anatomical structures and pathways of these areas. Although M1 motor pathways are critical, the premotor areas also contribute to motor control and might be recruited during motor recovery after stroke. The parallel nature of the direct (corticospinal) pathways from premotor areas and M1 emphasizes that PMd and SMA are, in some respects, at a similar level of hierarchical organization as M1[7], although these projections to spinal cord motor neurons are less numerous and less efficient that those from M1[8-10]. Another possibility is the indirect (corticoreticulospinal) projections to cervical propriospinal premotoneurons, which have divergent projections to muscle groups operating at multiple joints[11, 12]. Finally, cortico-cortical connections between these areas might also play an important role in post-stroke recovery[7, 13-15]. Thus, understanding the neural events associated with the functional changes in these areas could provide critical insight into successful treatments of patient's impairment.

Proton magnetic resonance spectroscopy ($^{1}$H-MRS) provides a non-invasive means to measure concentrations of certain metabolites associated with a specific cell type[16] after stroke[17]. Most clinical stroke studies report lower levels of N-acetylaspartate (NAA, putative marker of neuronal integrity) in spared ipsilesional M1 and PMd[18-21]. In some instances, the NAA levels were related to clinical severity. In a series of studies of stroke survivors, we also found higher myo-inositol (mI, putative marker of glial cells) in ipsilesional and contralesional M1[21]. However, none of these studies addressed the changes in key metabolites related to neuronal and glial compartments, i.e., NAA and mI, in motor and premotor areas in stroke.

The first aim of the current study was to quantify NAA and mI concentrations in ipsilesional and contralesional motor and pre-motor areas in chronic subcortical stroke. Since neuronal integrity might be compromised in these remote areas[21, 22], we expected NAA to be lower, especially in the ipsilesional areas. Given the role of glia in plastic brain changes[23-25], we also expected mI to be higher. The second aim was to explore correlations between metabolite concentrations and arm motor impairment. Since the premotor projections are significantly stronger on the proximal muscles than distal muscles compared to M1[8, 9], we predicted that metabolite measures in ipsilesional PMd and SMA would be correlated with proximal (shoulder/elbow) motor impairment whereas those in M1 would be correlated with both proximal and distal (hand) impairments. Since both direct and indirect pathways from the contralesional M1 project to axial and proximal muscles rather than hand muscles[26, 27],

relationships between contralesional M1 metabolites and proximal impairment were also expected.

## Materials and Methods

### Participants

Twenty stroke participants and sixteen healthy controls (all right-handed and without MRI contraindications) signed informed consent in accordance with the University of Kansas Medical Center Human Subjects Committee (Institutional Review Board) prior to their recruitment in the study.

Patients were included if they had (i) a single ischemic subcortical stroke more than six months prior to study recruitment, (ii) radiologically-normal appearing motor and premotor areas based on T2-weighted magnetic resonance imaging (MRI), (iii) ability to understand consenting (Token test), (iv) no visual attention deficits (Cancellation test), apraxia (clinical observation of the use of scissors to cut paper and making coffee), or other chronic or degenerative neurological disease (medical chart review). Stroke survivors were on anti-hypertensive (95%), cholesterol-lowering (45%) and/or antiplatelet (45%) therapy, but were not receiving inpatient or outpatient treatment.

Age-, sex-, and education-matched healthy controls, with normal T2-weighted MRI and without neurological and psychiatric disorders, were recruited.

### Data acquisition

MRI studies were conducted on a 3T Allegra MR system (Siemens Medical Solutions, Erlangen, Germany). Each participant's head was immobilized with head cushions. Our experimental protocol has been detailed previously [21]. In short, an axial proton density/T2-weighted MRI (TR=4800ms; TE1/TE2=18/106ms; FOV=240mm; matrix=256×256; slice thickness=5mm, no gap) and a whole-brain 3D T1-weighted MRI (TR=2300ms; TE=3ms; FOV=240mm; matrix=256×256; resolution=1×1×1mm$^3$) were acquired to confirm the location of a single lesion that did not involve the motor and premotor areas and to estimate the brain tissue volume in spectroscopic voxels respectively. A gradient echo blood oxygen level-dependent scan (BOLD; TR=2000ms; TE=50ms; FOV=240mm; matrix=64×64; slice thickness=5mm; 0 skip; resolution=5×5mm$^2$; 100 time points) was acquired to identify the hand representation area within our regions of interest (ROI), M1, PMd, and SMA, in each hemisphere. For BOLD scans, two alternating conditions were repeated: movement (20s), where participants performed a handgrip with the impaired hand (dominant in controls) until a target pressure (25% of handgrip maximal voluntary contraction) was attained; and rest (20s), where participants were motionless. BOLD scanning lasted for a total of 3min 28s.

BOLD data were analyzed initially using the scanner analysis software to guide the $^1$H-MRS imaging ($^1$H-MRSI) slab positioning. Specifically, the slices corresponding to the activated motor/premotor areas were used to select the corresponding coincident T2-weighted image upon which the $^1$H-MRSI slab was centered. The $^1$H-MRSI volume of interest was placed in the frontal and parietal lobes including our ROIs, parallel to the anterior commissure-posterior commissure line, and positioned with the bottom edge of the slab at the cingulate sulcus and the anterior edge aligned with the anterior tip of the genu. $^1$H-MRSI was acquired using a point-resolved spectroscopy sequence (PRESS; TE=30ms; TR=1500ms; FOV=160mm$^2$; matrix=16×16; slice thickness=15mm; in-plane resolution=5×5mm$^2$; spectral width=1200Hz). Scalp lipid artifact was minimized with eight 30mm outer voxel suppression bands prescribed around the $^1$H-MRSI excitation volume. Automated and manual shimming yielded an optimal full-width at half maximum of < 20Hz of the water signal from the entire excitation volume.

### Analysis of functional imaging data

We analyzed BOLD using Brain Voyager software (Brain Innovation B.V., Maastricht, Netherlands). Motion correction was performed using a rigid body transformation, estimating six parameters (three translational and three rotational). Inspection of these parameters found that none of the participants moved their head more than 2mm in any direction. Then, 3D spatial smoothing with a 4mm Gaussian filter was used to permit valid statistical inferences based on Gaussian random field theory. The time series in each voxel was high-pass filtered at 0.01Hz to remove low frequency confounds. Movement and rest periods were modeled by a boxcar function with hemodynamic response modification (predictor movement) and the general linear model was used to extract foci of activation in each ROI (cluster threshold=100 voxels, $p_{Bonferroni}$=0.01). Then, we outlined ROIs on the background T1 image using standard sulcal and gyral landmarks[28], i.e., without knowledge of the activation patterns: M1, on the anterior bank of the central sulcus with the caudal border lying in the depth of the central sulcus close to its fundus and anterior border abutting area 6; PMd, on the anterior half of the precentral gyrus; SMA, on the medial wall of the hemisphere from the top of the brain to the depth of the cingulated sulcus, between a posterior boundary, halfway between the extension of the central and precentral sulci onto the medial surface, and an anterior boundary, a vertical line through the anterior commissure. We then counted the activated voxels in the ROI using a Bonferroni corrected p=0.01/total voxels in the ROI, as defined by BV software. The ratio (expressed as a %) between the number of activated voxels and the total number of voxels in the ROI represents the spatial extent of activation.

### Analysis of spectroscopic imaging data

$^{1}$H-MRSI data were quantified using LCModel (linear combination of model spectra using a basis set included in the package and using a radio-frequency coil loading factor[29]). We also segmented the T1-weighted images using SPM2 (Welcome Department of Cognitive Neurology, London, UK) into white matter (WM), grey matter (GM), and cerebral spinal fluid (CSF).

Then, to select the spectroscopic voxels in the relevant regions of M1, PMd, and SMA associated with motor output, we overlaid the BOLD images, quantitative spectroscopic output (LCModel), and segmented T1-weighted images (SPM2) using custom-designed software (Matlab v7.1). This graphical interface was used to display spectra and to obtain metabolite concentrations and brain tissue fraction from selected spectroscopic voxels. We selected three spectroscopic voxels per ROI (Fig. 1), each with a signal-to-noise ratio greater than 10 and with more than 75% GM.

The metabolites of interest, NAA and mI, were included in the quantitative analysis if their Cramer-Rao lower bounds were lower than 20% in all spectra. Since the metabolites have different concentrations in brain tissue (BT) and CSF, we corrected the concentrations as follows: c=cLCModel/BT where c is the BT-corrected concentration, cLCModel is the concentration in institutional unit from LCModel output, and BT is the estimated brain tissue i.e., WM+GM from the SPM segmentation. BT-corrected concentration was then converted into molar concentrations (millimoles per kilogram wet weight brain tissue)[21].

In the stroke group, we selected the FMUE components specifically dealing with distal movements, including hand movements (distal subscore, normal=14) and proximal movements, including active shoulder and elbow movements in and out of synergy (proximal subscore, normal=30), to evaluate distal and proximal arm motor impairments.

### Statistical analysis

Metabolite concentrations were described by means and standard deviations and the between-group differences in mean concentrations were expressed as percent change of the control group (see Fig. 2A) for illustration purpose. The percent change was computed as follows: %metabolite change = (mean $\text{metabolite}_{\text{stroke}}$ − mean $\text{metabolite}_{\text{control}}$) × 100 / mean $\text{metabolite}_{\text{control}}$.

For inference, we used mixed-effects models to compare metabolite concentrations in each ROI within and between groups. Least-square means were used to assess the differences in metabolite concentrations between M1 and PMd or M1 and SMA within each hemisphere in each group (2 comparisons/metabolite/hemisphere × 2 hemispheres × 2 metabolites = 8 comparisons). Finally, group-by-ROI interactions were employed to evaluate between-ROI differences in each hemisphere between groups (2 between-ROI differences/hemisphere/metabolite × 2 hemispheres × 2 metabolites = 8 interactions).

In the stroke group, relationships between metabolite concentrations and FMUE subscores were analyzed with Spearman Rank Order correlation test.

Significant differences were considered at $p<0.05$ (SPSS 18.0, SPSS Inc. Chicago, IL, except the mixed-effects analysis which was performed on SAS 9.2, SAS Inc. Cary, NC). Corrections for multiple comparisons were not performed in this exploratory study.

## Results

### Participants

Stroke participants characteristics are listed in Table 1. Patients (13 male/7 female, age range 36 to 73 years, mean±SD, 57.3±10.3 years) having a single subcortical infarction were recruited at 6 to 144 months (44.6±37.8 months) post-injury. The site of cerebral infarction was determined from T2-weighted MRI[30]. Twelve patients had experienced right hemiparesis and eight left hemiparesis. Seventeen patients had experienced infarcts involving the striato-capsular area. Of these, three were found to have anterior limb of internal capsule involvement, seven posterior limb, three both anterior and posterior limbs of internal capsule, and six striato-capsular infarcts with extension to the corona radiata. In addition, two patients had suffered from pontine infarctions (pons), and one from infarction of the posterior cerebral artery territory involving the cerebral peduncles. Patients had proximal and distal motor deficits in their impaired arm based on the FMUE subscores (Table 1).

The age of healthy controls (10 male/6 female) ranged from 36 to 74 years (49.4±14.7 years). Stroke and control groups did not differ statistically with respect to age ($p>0.05$), sex (65% vs. 63% male), or education (13.6±2.0 vs. 14.7±3.2 years, $p>0.05$).

### Spectral quality

All spectra in each group showed a high signal-to-noise ratio (>10 from LCModel). Similar percentages of BT within spectroscopic voxels were found in each group (ipsilesional vs. left: M1, 89.3±5.8% vs. 89.4±6.5%, p=0.9; PMd, 85.9±7.4% vs. 89.8±8.1%, p=0.1; contralesional vs. right: M1, 86.7±8.4% vs. 86.2±4.9%, p=0.8; PMd, 85.8±8.9% vs. 84.9±6.4%, p=0.7; SMA, 82.2±7.3 vs. 85.1±5.8%, p=0.7) although the BT fraction in ipsilesional SMA was slightly higher in patients (81.3±4.4% vs. 77.6±4.3%, p=0.02).

### Spectroscopic voxel location

Although larger motor-related activations were found in patients compared with controls (Table 2), the anatomical locations of spectroscopic voxels were similar between groups. Typical examples of voxel location for the three ROIs are shown in Fig. 1.

### Metabolite concentrations

**Healthy Controls—**Comparing motor areas within each hemisphere, we found that mI was higher in SMA than in M1 (left, $p<0.0001$; right, $p=0.0002$). NAA was not different between ROIs. Overall, no significant differences in any metabolite concentrations were detected between left and right motor cortices ($p>0.05$) in healthy brains.

**Stroke Participants—**Within each hemisphere, similar to healthy controls, mI concentrations were higher in SMA than in M1 (ipsilesional, $p=0.002$; contralesional, $p=0.006$). NAA concentrations were similar across ROIs. Similar to controls, in patients, comparable metabolite concentrations were found between ipsilesional and contralesional homologous areas.

**Comparisons between Stroke and Healthy Controls—**Since there were no lateralization differences in metabolite concentrations in controls, and most patients (12 out of 20) had left-sided infarcts, we compared metabolites in the ipsilesional hemisphere with left-hemisphere metabolites from controls. Table 3 shows between-group differences in metabolite concentrations within each ROI. Across all ROIs, NAA concentrations were generally lower and mI generally higher in stroke survivors than in controls (Table 3 and Fig. 2A). Not surprisingly, these findings were more prominent, and reached statistical significance, in ipsilesional ROIs: NAA was lower in M1 (by 10.7%, $p=0.04$) and SMA (13.9%, $p=0.004$); mI was higher in M1 (21.4%, $p=0.003$) and PMd (15.2%, $p=0.03$). Subgroup analysis of those patients with lesions of the posterior limb of the internal capsule ($n=7$) showed lower NAA in M1 (by 16.9%, $p=0.02$), PMd (14.8%, $p=0.03$), and SMA (20.8%, $p=0.01$) and higher mI in M1 (21.7%, $p=0.001$) in the ipsilesional hemisphere.

### Correlations between metabolite concentrations and arm motor impairment

Significant correlations were found between ipsilesional NAA and hand (M1, $r=0.51$, $p=0.04$) and shoulder/elbow (M1, $r=0.55$, $p=0.02$; PMd, $r=0.51$, $p=0.01$; SMA, $r=0.51$, $p=0.02$) FMUE subscores (Fig. 2B). Contralesional M1 NAA was significantly correlated with shoulder/elbow FMUE subscores ($r=0.54$, $p=0.02$). There were no significant correlations between ipsilesional or contralesional mI concentrations and FMUE subscores.

## Discussion

We used non-invasive magnetic resonance spectroscopy to investigate the effects of an ischemic subcortical stroke on metabolites related to neurons and glia in spared motor and premotor areas. We also investigated the relationships between these metabolites and the clinical severity of arm motor impairment. We found altered metabolite concentrations, i.e., lower NAA and higher mI, across ipsilesional motor and premotor areas. Ipsilesional NAA values were correlated with proximal and distal arm motor impairments while contralesional motor NAA with proximal impairment.

### Stroke-related metabolite alterations in spared motor and premotor cortices

The magnitude of the metabolite alterations described here is similar to spectroscopic findings in normal-appearing brain tissue in other central nervous system (CNS) pathologies such as systemic lupus erythematous [31], traumatic brain injury [32], multiple sclerosis [33, 34],

and Alzheimer's disease [35]. Accordingly, although the physiological mechanisms might differ, we consider the changes in NAA and mI reported in our patients to be biologically robust.

Since NAA is found almost exclusively in neurons[36], lower concentrations in ipsilesional M1 and SMA might be due to neuronal loss[37] and/or neuronal mitochondrial depression[21, 22]. On the one hand, irreversible neuronal loss seems unlikely since few data regarding retrograde degeneration[38] or remote apoptotic cell death have been reported after stroke. On the other hand, within remote hypoperfused brain territory (middle cerebral artery territory in 95% of our patients), unless the recanalization or collateral blood supply is sufficient to prevent ischemia[39], multiple remote focal infarctions may occur. This may partially explain low NAA in ipsilesional M1 (and in ipsilesional PMd in the subgroup of patients with lesions of the posterior limb of the internal capsule) but not in ipsilesional SMA (supplied by anterior cerebral artery). Moreover, if neuronal loss was significant, cortical volume loss might be expected, but we found percentages of brain tissue volume measured in the spectroscopic voxels to be similar in patients and controls. Therefore, appreciable remote neuronal death seems unlikely. However, these areas might contain neurons with "damaged" axons, since subcortical stroke is likely to involve both motor and premotor pathways[40, 41]. Indeed, after axonal injury, morphological and biochemical cell body changes produce shifting from a "transmitting" to a "degenerative/regenerative" state causing neuronal depression[38, 42]. In our sample, the anterior limb of the internal capsule was involved in 15% of patients, the posterior limb in 35% of patients and both anterior and posterior limbs in 15% of patients. Although the majority of premotor efferents course through the anterior limb and genu of the internal capsule[43] those efferents relevant for arm recovery *per se* generally course more posteriorly through the posterior limb[40, 41]. Indeed, our subgroup analysis on patients with lesions of the posterior limb of the internal capsule showed notably lower NAA not only in M1 but also in PMd and SMA. Hence, our data could reflect the events that occur in remote motor and premotor neurons with "damaged" axons at the subcortical level. However, since only three patients suffered anterior limb lesions, we could not draw strong conclusions.

Currently, only one other study reported lower NAA in ipsilesional motor and premotor (PMd) areas after stroke[20]. Our findings of lower NAA in M1 and PMd corroborates the findings of Kobayashi et al, although the magnitude of our results in PMd for the entire group of patients is lower. This may reflect methodological differences, e.g., the use of white matter NAA/creatine ratios[20], or the fact that we studied chronic survivors of an ischemic subcortical stroke (> six months post-onset) compared to acute deep intracerebral (thalamus, putamen) hemorrhagic stroke (< one month) in their study.

We also report higher mI concentrations in ipsilesional M1 and PMd. These results confirm the findings of our previous report on 14 patients, that suggested higher mI in ipsilesional M1[21]. Since glial cells contain high concentrations of mI[37], reactive gliosis secondary to neuronal loss could explain elevated mI, but we found little evidence of neuronal death in these areas. Based on the role of the astrocytes in modulating synaptic transmission, synaptogenesis, and synaptic plasticity[23, 24, 44, 45], we hypothesize that glia may play an important role in brain plasticity after stroke. Indeed, a direct relationship between astroglial and synaptic responses post-stroke has been found in spared cortical areas[46]. Nonetheless, the specific mechanism underlying the altered mI concentrations remains an open question.

## Clinical correlations

In our study, patients with poorer proximal recovery were more likely to have low NAA suggesting altered neuronal integrity in contralesional M1 and ipsilesional M1, PMd, and SMA. In explaining these results, it is useful to consider the high degree of similarity

between the corticospinal projections from the hand regions of M1, PMd, and SMA[8-10], thus providing the substrate whereby motor areas acting in parallel could generate an output necessary for movement. This implies that damage in one of these areas could be at least partially compensated by recruitment of another.

Abnormal proximal movements of the arm are directly related to the use of compensatory behavior, i.e., new motor patterns resulting from the adaptation of remaining motor elements, in hemiparetic patients[47, 48]. Our group as well as others suggests that the neural systems mediating such behavior are likely to include remaining intact brain tissue in both hemispheres[49-53]. Concordant with these findings, our data may suggest that compensatory behavior is related to the neuronal integrity in spared contralesional motor and ipsilesional motor and premotor areas. This result has important implications for neuro-rehabilitation. Given that motor function could be altered through rehabilitative interventions, e.g., electromagnetic stimulation[54, 55], preventive or permissive strategies for compensatory behavior could be developed.

### Study limitations

There are several limitations to this study. First, although our focus on subcortical infarcts provides statistical power by minimizing patient variance, it limits our ability to explore the effects of infarct location on metabolite concentrations (e.g., subcortical vs. cortical). Second, our sample included a wide range of time after injury (6 to 144 months). This might have contributed to the spread of metabolite concentrations, although no data regarding the evolution of metabolites in remote areas over such a long period have been reported. Third, our results (lower NAA) could be explained, in part, by cerebral blood flow alterations, perhaps resulting from carotid stenosis. However, there is some evidence that reduced blood flow also results in elevated choline and lactate[56-59]. Since we did not observe alterations in these two metabolites, we consider that carotid stenosis is not an appreciable contributor to our findings. Fourth, it is difficult to rule out contributions of plasticity occurring elsewhere within the network. Future studies are required to determine the relative contributions of different sites of plasticity and the experimental conditions in which they apply differentially. Finally, due to the point-spread function of $^{1}$H-MRSI acquisitions, the effective voxel size is bigger than the nominal voxel size. Thus, we cannot rule out the possibility that our measurements include more than hand representation in each area.

## Conclusions

We promote the use of the cutting-edge MRS measurements to improve our understanding of the neural substrates underlying reorganization in remaining intact brain structures after stroke. Such an approach may further enable monitoring recovery or compensation based on this reorganization and evaluating new treatment regimes that assist motor recovery.

## Acknowledgments

This work was supported by American Heart Association (0860041Z to Dr. Cirstea; 0655759Z to Dr. Brooks). The Hoglund Brain Imaging Center is supported by a generous gift from Forrest and Sally Hoglund and funding from the National Institutes of Health (P30 HD002528, S10 RR29577, UL1 RR033179, and P30 AG035982). Dr. Brooks is also supported in part by P30 AG035982, R01 AG033673, R01 DK080090, R01 DK085605, and UL1 RR033179. Dr. Nudo is supported in part R37 NS030853. The content is solely the responsibility of the authors and does not necessarily represent the official views of the funding agencies.

## References

1. Cramer SC. Repairing the human brain after stroke: I. Mechanisms of spontaneous recovery. Ann Neurol. 2008; 63:272–87. [PubMed: 18383072]

2. Ward NS, Brown MM, Thompson AJ, Frackowiak RS. Neural correlates of outcome after stroke: A cross-sectional fmri study. Brain. 2003; 126:1430–1448. [PubMed: 12764063]
3. Gerloff C, Bushara K, Sailer A, Wassermann EM, Chen R, Matsuoka T, Waldvogel D, Wittenberg GF, Ishii K, Cohen LG, Hallett M. Multimodal imaging of brain reorganization in motor areas of the contralesional hemisphere of well recovered patients after capsular stroke. Brain. 2006; 129:791–808. [PubMed: 16364955]
4. Marshall RS, Perera GM, Lazar RM, Krakauer JW, Constantine RC, DeLaPaz RL. Evolution of cortical activation during recovery from corticospinal tract infarction. Stroke. 2000; 31:656–61. [PubMed: 10700500]
5. Calautti C, Baron JC. Functional neuroimaging studies of motor recovery after stroke in adults: A review. Stroke. 2003; 34:1553–66. [PubMed: 12738893]
6. Ward NS, Brown MM, Thompson AJ, Frackowiak RS. Neural correlates of motor recovery after stroke: A longitudinal fmri study. Brain. 2003; 126:2476–96. [PubMed: 12937084]
7. Dum RP, Strick PL. Motor areas in the frontal lobe of the primate. Physiol Behav. 2002; 77:677–82. [PubMed: 12527018]
8. Boudrias MH, Lee SP, Svojanovsky S, Cheney PD. Forelimb muscle representations and output properties of motor areas in the mesial wall of rhesus macaques. Cerebral Cortex. 2010; 20:704–19. [PubMed: 19633176]
9. Boudrias MH, McPherson RL, Frost SB, Cheney PD. Output properties and organization of the forelimb representation of motor areas on the lateral aspect of the hemisphere in rhesus macaques. Cerebral Cortex. 2010; 20:169–86. [PubMed: 19561063]
10. Maier MA, Armand J, Kirkwood PA, Yang HW, Davis JN, Lemon RN. Differences in the corticospinal projection from primary motor cortex and supplementary motor area to macaque upper limb motoneurons: An anatomical and electrophysiological study. Cerebral Cortex. 2002; 12:281–96. [PubMed: 11839602]
11. Mazevet D, Meunier S, Pradat-Diehl P, Marchand-Pauvert V, Pierrot-Deseilligny E. Changes in propriospinally mediated excitation of upper limb motoneurons in stroke patients. Brain. 2003; 126:988–1000. [PubMed: 12615654]
12. Stinear JW, Byblow WD. The contribution of cervical propriospinal premotoneurons in recovering hemiparetic stroke patients. J Clin Neurophysiol. 2004; 21:426–34. [PubMed: 15622129]
13. Boussaoud D, Tanne-Gariepy J, Wannier T, Rouiller EM. Callosal connections of dorsal versus ventral premotor areas in the macaque monkey: A multiple retrograde tracing study. BMC Neurosci. 2005; 6:67. [PubMed: 16309550]
14. Marconi B, Genovesio A, Giannetti S, Molinari M, Caminiti R. Callosal connections of dorso-lateral premotor cortex. European J Neuroscience. 2003; 18:775–88.
15. Mochizuki H, Huang YZ, Rothwell JC. Interhemispheric interaction between human dorsal premotor and contralateral primary motor cortex. J Physiol. 2004; 561:331–8. [PubMed: 15459244]
16. Van Zijl PC, Barker PB. Magnetic resonance spectroscopy and spectroscopic imaging for the study of brain metabolism. Ann N Y Acad Sci. 1997; 820:75–96. [PubMed: 9237450]
17. Saunders DE. MR spectroscopy in stroke. Br Med Bull. 2000; 56:334–45. [PubMed: 11092084]
18. Munoz, Maniega S.; Cvoro, V.; Chappell, FM.; Armitage, PA.; Marshall, I.; Bastin, ME.; Wardlaw, JM. Changes in naa and lactate following ischemic stroke: A serial mr spectroscopic imaging study. Neurology. 2008; 71:1993–9. [PubMed: 19064881]
19. Kang DW, Roh JK, Lee YS, Song IC, Yoon BW, Chang KH. Neuronal metabolic changes in the cortical region after subcortical infarction: A proton mr spectroscopy study. J Neurol Neurosurg Psychiatry. 2000; 69:222–7. [PubMed: 10896697]
20. Kobayashi M, Takayama H, Suga S, Mihara B. Longitudinal changes of metabolites in frontal lobes after hemorrhagic stroke of basal ganglia: A proton magnetic resonance spectroscopy study. Stroke. 2001; 32:2237–45. [PubMed: 11588307]
21. Cirstea MC, Brooks WM, Craciunas SC, Popescu AE, Choi I, Lee S, Bani-Ahmed A, Yeh H, Savage CR, Cohen LG, Nudo RJ. Primary motor cortex - a functional mri-guided proton magnetic resonance spectroscopic study. Stroke. 2011; 42:1004–9. [PubMed: 21330627]

22. Chu WJ, Mason GF, Pan JW, Hetherington HP, Liu HG, San Pedro EC, Mountz JM. Regional cerebral blood flow and magnetic resonance spectroscopic imaging findings in diaschisis from stroke. Stroke. 2002; 33:1243–8. [PubMed: 11988598]
23. Henneberger C, Papouin T, Oliet SH, Rusakov DA. Long-term potentiation depends on release of d-serine from astrocytes. Nature. 2010; 463:232–6. [PubMed: 20075918]
24. Rango M, Cogiamanian F, Marceglia S, Barberis B, Arighi A, Biondetti P, Priori A. Myoinositol content in the human brain is modified by transcranial direct current stimulation in a matter of minutes: A 1h-mrs study. Magn Reson Med. 2008; 60:782–9. [PubMed: 18816828]
25. Shibuya M. Brain angiogenesis in developmental and pathological processes: Therapeutic aspects of vascular endothelial growth factor. FEBS J. 2009; 276:4636–43. [PubMed: 19664071]
26. Brinkman J, Kuypers HG. Cerebral control of contralateral and ipsilateral arm, hand and finger movements in the split-brain rhesus monkey. Brain. 1973; 96:653–74. [PubMed: 4204228]
27. Carr LJ, Harrison LM, Stephens JA. Evidence for bilateral innervation of certain homologous motoneurone pools in man. J Physiology. 1994; 475:217–27.
28. Constable RT, Skudlarski P, Mencl E, Pugh KR, Fulbright RK, Lacadie C, Shaywitz SE, Shaywitz BA. Quantifying and comparing region-of-interest activation patterns in functional brain mr imaging: Methodology considerations. Magn Reson Imaging. 1998; 16:289–300. [PubMed: 9621970]
29. Provencher SW. Automatic quantitation of localized in vivo 1h spectra with lcmodel. NMR Biomed. 2001; 14:260–4. [PubMed: 11410943]
30. Mai, JK.; Paxinos, G.; Voss, T. Atlas of the human brain. Elsevier; New York, NY: 2008.
31. Sabet A, Sibbitt WL Jr. Stidley CA, Danska J, Brooks WM. Neurometabolite markers of cerebral injury in the antiphospholipid antibody syndrome of systemic lupus erythematosus. Stroke. 1998; 29:2254–60. [PubMed: 9804631]
32. Garnett MR, Blamire AM, Rajagopalan B, Styles P, Cadoux-Hudson TA. Evidence for cellular damage in normal-appearing white matter correlates with injury severity in patients following traumatic brain injury: A magnetic resonance spectroscopy study. Brain. 2000; 123:1403–9. [PubMed: 10869052]
33. Chard DT, Griffin CM, McLean MA, Kapeller P, Kapoor R, Thompson AJ, Miller DH. Brain metabolite changes in cortical grey and normal-appearing white matter in clinically early relapsing-remitting multiple sclerosis. Brain. 2002; 125:2342–52. [PubMed: 12244090]
34. Sastre-Garriga J, Ingle GT, Chard DT, Ramio-Torrenta L, McLean MA, Miller DH, Thompson AJ. Metabolite changes in normal-appearing gray and white matter are linked with disability in early primary progressive multiple sclerosis. Archives Neurology. 2005; 62:569–73.
35. Watanabe T, Shiino A, Akiguchi I. Absolute quantification in proton magnetic resonance spectroscopy is useful to differentiate amnesic mild cognitive impairment from alzheimer's disease and healthy aging. Dement Geriatr Cogn Disord. 2010; 30:71–7. [PubMed: 20689286]
36. Baslow MH. N-acetylaspartate in the vertebrate brain: Metabolism and function. Neurochem Res. 2003; 28:941–53. [PubMed: 12718449]
37. Siegel, GJB.; Agranoff, BW.; Albers, GW.; Fisher, SK.; Uhler, MD. Basic Neurochemistry: Molecular, Cellular, Medical Aspects. Academic Press; Oxford, UK: 2005.
38. Wannier T, Schmidlin E, Bloch J, Rouiller EM. A unilateral section of the corticospinal tract at cervical level in primate does not lead to measurable cell loss in motor cortex. J Neurotrauma. 2005; 22:703–17. [PubMed: 15941378]
39. Seitz RJ, Donnan GA. Role of neuroimaging in promoting long-term recovery from ischemic stroke. J Magn Reson Imaging. 2010; 32:756–72. [PubMed: 20882606]
40. Shelton FN, Reding MJ. Effect of lesion location on upper limb motor recovery after stroke. Stroke. 2001; 32:107–12. [PubMed: 11136923]
41. Werring DJ, Clark CA, Barker GJ, Miller DH, Parker GJ, Brammer MJ, Bullmore ET, Giampietro VP, Thompson AJ. The structural and functional mechanisms of motor recovery: Complementary use of diffusion tensor and functional magnetic resonance imaging in a traumatic injury of the internal capsule. J Neurol Neurosurg Psychiatry. 1998; 65:863–9. [PubMed: 9854962]
42. Lieberman AR. The axon reaction: A review of the principal features of perikaryal responses to axon injury. Int Rev Neurobiol. 1971; 14:49–124. [PubMed: 4948651]

43. Fries W, Danek A, Scheidtmann K, Hamburger C. Motor recovery following capsular stroke. Role of descending pathways from multiple motor areas. Brain. 1993; 116:369–82.
44. Ullian EM, Sapperstein SK, Christopherson KS, Barres BA. Control of synapse number by glia. Science. 2001; 291:657–61. [PubMed: 11158678]
45. Jones, TA.; Greenough, WT. Behavioral experience-dependent plasticity of glial-neuronal interactions. In: Volterra, A.; Magistretti, PJ.; Haydon, PG., editors. The tripartite synapse: Glia in synaptic transmission. Oxford University Press; New York: 2002. p. 248-56.
46. Kim SY, Jones TA. Lesion size-dependent synaptic and astrocytic responses in cortex contralateral to infarcts in middle-aged rats. Synapse. 2010; 64:659–71. [PubMed: 20336630]
47. Cirstea MC, Levin MF. Compensatory strategies for reaching in stroke. Brain. 2000; 123:940–53. [PubMed: 10775539]
48. Raghavan P, Santello M, Gordon AM, Krakauer JW. Compensatory motor control after stroke: An alternative joint strategy for object-dependent shaping of hand posture. J Neurophysiology. 2010; 103:3034–43.
49. Metz GA, Antonow-Schlorke I, Witte OW. Motor improvements after focal cortical ischemia in adult rats are mediated by compensatory mechanisms. Behav Brain Res. 2005; 162:71–82. [PubMed: 15922067]
50. Eisner-Janowicz I, Barbay S, Hoover E, Stowe AM, Frost SB, Plautz EJ, Nudo RJ. Early and late changes in the distal forelimb representation of the supplementary motor area after injury to frontal motor areas in the squirrel monkey. J Neurophysiology. 2008; 100:1498–512.
51. Nishibe M, Barbay S, Guggenmos D, Nudo RJ. Reorganization of motor cortex after controlled cortical impact in rats and implications for functional recovery. J Neurotrauma. 2010; 27:2221–32. [PubMed: 20873958]
52. Riecker A, Groschel K, Ackermann H, Schnaudigel S, Kassubek J, Kastrup A. The role of the unaffected hemisphere in motor recovery after stroke. Human Brain Mapping. 2010; 31:1017–29. [PubMed: 20091792]
53. Lee MY, Park JW, Park RJ, Hong JH, Son SM, Ahn SH, Cho YW, Jang SH. Cortical activation pattern of compensatory movement in stroke patients. NeuroRehabilitation. 2009; 25:255–60. [PubMed: 20037218]
54. Hamada M, Hanajima R, Terao Y, Okabe S, Nakatani-Enomoto S, Furubayashi T, Matsumoto H, Shirota Y, Ohminami S, Ugawa Y. Primary motor cortical metaplasticity induced by priming over the supplementary motor area. J Physiology. 2009; 587:4845–62.
55. Nowak DA, Grefkes C, Ameli M, Fink GR. Interhemispheric competition after stroke: Brain stimulation to enhance recovery of function of the affected hand. Neurorehabil Neural Repair. 2009; 23:641–56. [PubMed: 19531606]
56. van der Grond J, Balm R, Klijn CJ, Kapelle LJ, Eikelboom BC, Mali WP. Cerebral metabolism of patients with stenosis of the internal carotid artery before and after endarterectomy. J Cereb Blood Flow Metab. 1996; 16:320–6. [PubMed: 8594065]
57. Hattingen E, Lanfermann H, Menon S, Neumann-Haefelin T, de Rochement RD, Stamelou M, Hoglinger GU, Magerkurth J, Pilatus U. Combined 1h and 31p mr spectroscopic imaging: Impaired energy metabolism in severe carotid stenosis and changes upon treatment. Magma. 2009; 22:43–52. [PubMed: 18855032]
58. Walker PM, Ben Salem D, Giroud M, Brunotte F. Is naa reduction in normal contralateral cerebral tissue in stroke patients dependent on underlying risk factors? J Neurology, Neurosurgery, Psychiatry. 2006; 77:596–600.
59. Zhang M, Lu J, Jiao L, Ma Q, Li K. Proton magnetic resonance spectroscopy in patients with symptomatic unilateral internal carotid artery / middle cerebral artery stenosis or occlusion. J Magn Reson Imaging. 2011; 34:910–6. [PubMed: 21774028]

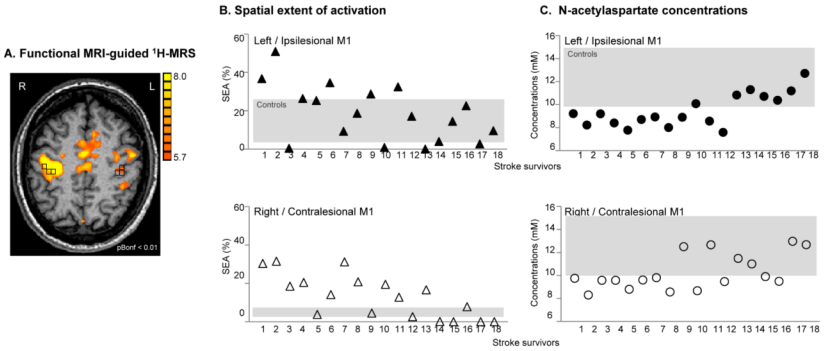


**Fig. 1.**

Motor-related cortical activation during a handgrip task executed with the impaired right hand in a 58-age old patient who had experienced infarct involving the left striato-capsular area (Patient 18, Table 1). $^{1}$H-MRSI slab (grey rectangle) was positioned on axial T1-weigthed MR image at the level of motor-related motor/premotor activation. Spectroscopic voxels (black squares) were selected based on M1, PMd, and SMA activation (or anatomical landmarks in case the activation tended to zero). L=left, R=right

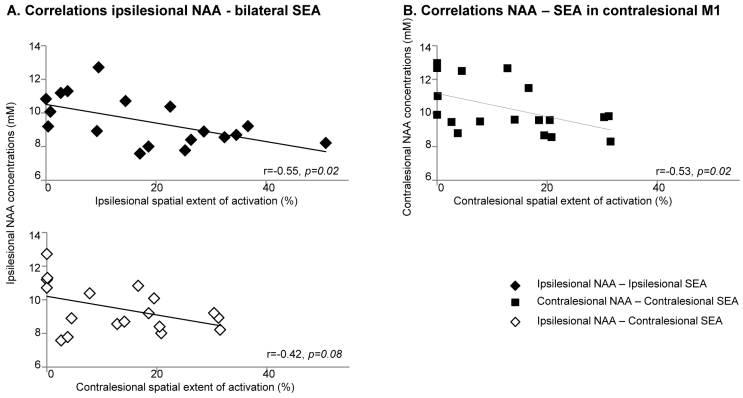


**Fig. 2.**

**A.** Changes (%) in concentrations of NAA (black) and mI (light grey) in M1, PMd, and SMA in both hemispheres in stroke survivors versus controls. Note that NAA is lower in ipsilesional M1 (*p=0.04*) and SMA (*p=0.004*) and mI is higher in M1 (*p=0.003*) and PMd (*p=0.03*). **B**. Correlations between NAA concentrations in contralesional M1 (black circle), ipsilesional M1 (diamond), ipsilesional PMd (triangle), and ipsilesional SMA (square) and proximal FMUE subscores.

## Table 1

Stroke participants demographic and clinical characteristics

| Age (years) | Sex | Time to scan (mo) | Site of lesion | *Proximal arm motor impairment | *Distal arm motor impairment |
|---|---|---|---|---|---|
| 57 | M | 6 | L MCA - SC, CR | 30 | 14 |
| 68 | M | 63 | L MCA - SC | 30 | 14 |
| 46 | M | 52 | L MCA - SC | 26 | 14 |
| 48 | F | 11 | L MCA - SC | 26 | 14 |
| 46 | F | 8 | R MCA - SC | 26 | 13 |
| 61 | F | 27 | L MCA - SC | 26 | 14 |
| 56 | M | 23 | R Pons | 20 | 14 |
| 45 | M | 27 | R MCA - SC | 17 | 10 |
| 73 | M | 60 | R MCA - BG | 16 | 10 |
| 61 | M | 15 | L Pons | 16 | 6 |
| 63 | F | 48 | L Pons | 14 | 4 |
| 71 | M | 26 | L MCA - SC | 13 | 8 |
| 44 | F | 106 | L PCA - CP | 13 | 6 |
| 71 | M | 98 | L MCA - CR | 13 | 13 |
| 65 | M | 36 | R MCA - SC | 11 | 12 |
| 56 | F | 6 | R MCA - SC | 11 | 8 |
| 59 | M | 144 | R MCA - BG | 11 | 6 |
| 58 | M | 27 | L MCA - SC | 11 | 4 |
| 36 | F | 84 | R MCA - SC, CR | 7 | 2 |
| 61 | M | 24 | L MCA - SC | 5 | 1 |

M=male, F=female; mo=months; L=left, R=right; MCA=middle cerebral artery; PCA=posterior cerebral artery; SC=striato-capsular territory; CR=corona radiata; CP=cerebral peduncles; BG=basal ganglia.

*Proximal and distal arm motor impairment refers to the Fugl-Meyer Upper Extremity subscores (30 for normal shoulder and elbow movements in and out of synergy; 14 for normal hand movements) as recorded at the recruitment into study.

## Table 2

Spatial extent of motor-related BOLD activation (mean ± SD, %) within M1, PMd, and SMA, bilaterally measured, in control and stroke groups.

| | *Right / Contralesional hemisphere* | *Left / Ipsilesional hemisphere* |
|---|---|---|
| **M1** | | |
| Control | 0.9 ± 1.6 | 18.0 ± 12.3 |
| Stroke | 10.0 ± 11.4 | 25.9 ± 13.4 |
| *p-value* | *0.002* | *0.04* |
| **PMd** | | |
| Control | 0.6 ± 0.8 | 2.7 ± 3.5 |
| Stroke | 3.6 ± 4.3 | 9.3 ± 9.1 |
| *p-value* | *0.04* | *0.04* |
| **SMA** | | |
| Control | 1.2 ± 0.9 | 2.4 ± 1.8 |
| Stroke | 10.1 ± 8.6 | 21.5 ± 16.2 |
| *p-value* | *0.006* | *0.002* |

*p-value* signifies the difference between groups

## Table 3

Metabolite concentrations (mean ± SD, mM) within M1, PMd, and SMA, bilaterally measured, in control and stroke groups.

| | NAA | mI | NAA | mI |
|---|---|---|---|---|
| *Right / Contralesional hemisphere* | | | *Left / Ipsilesional hemisphere* | |
| **M1** | | | | |
| Control | 11.6 ± 2.0 | 5.1 ± 1.2 | 11.2 ± 1.7 | 4.9 ± 0.8 |
| Stroke | 10.7 ± 1.6 | 5.7 ± 1.1 | 10.0 ± 1.6 | 5.9 ± 1.1 |
| *p-value* | *0.2* | *0.1* | ***0.04*** | ***0.003*** |
| **PMd** | | | | |
| Control | 12.2 ± 1.9 | 5.8 ± 1.1 | 11.9 ± 2.2 | 5.4 ± 0.9 |
| Stroke | 11.6 ± 1.7 | 6.1 ± 1.3 | 10.9 ± 1.8 | 6.2 ± 1.3 |
| *p-value* | *0.3* | *0.4* | *0.09* | ***0.03*** |
| **SMA** | | | | |
| Control | 11.0 ± 2.3 | 6.2 ± 1.5 | 12.5 ± 2.1 | 6.7 ± 1.6 |
| Stroke | 10.2 ± 1.3 | 6.4 ± 1.3 | 10.7 ± 2.2 | 6.8 ± 1.2 |
| *p-value* | *0.2* | *0.6* | ***0.004*** | *0.8* |

*p-value* signifies the difference between groups